Evaluation of Geometric Modeling for KOMPSAT-1 EOC Imagery Using Ephemeris Data

Hong-Gyoo Sohn, Hwan-Hee Yoo, and Seong-Sam Kim

Using stereo images with ephemeris data from the Korea Multi-Purpose Satellite-1 electro-optical camera (KOMPSAT-1 EOC), we performed geometric modeling for three-dimensional (3-D) positioning and evaluated its accuracy. In the geometric modeling procedures, we used ephemeris data included in the image header file to calculate the orbital parameters, sensor attitudes, and satellite position. An inconsistency between the time information of the ephemeris data and that of the center of the image frame was found, which caused a significant offset in satellite position. This time inconsistency was successfully adjusted. We modeled the actual satellite positions of the left and right images using only two ground control points and then achieved 3-D positioning using the KOMPSAT-1 EOC stereo images. The results show that the positioning accuracy was about 12–17 m root mean square error (RMSE) when 6.6 m resolution EOC stereo images were used along with the ephemeris data and only two ground control points (GCPs). If more accurate ephemeris data are provided in the near future, then a more accurate 3-D positioning will also be realized using only the EOC stereo images with ephemeris data and without the need for any GCPs.

Keywords: KOMPSAT-1 EOC, geometric modeling, ephemeris data, 3-D positioning.

Manuscript received July 21, 2003; revised Dec. 2, 2003.

Hong-Gyoo Sohn (phone: +82 2 2123 2809, email: sohn1@yonsei.ac.kr) is with School of Civil and Environmental Engineering, Yonsei University, Seoul, Korea.

Hwan-Hee Yoo (email: hhyoo@nongae.gsnu.ac.kr) and Seong-Sam Kim (email: kimss333@netian.com) are with the Department of Urban Engineering, ERDI, Gyeongsang National University, Jinju, Korea.

I. Introduction

The usefulness of a spacecraft program in providing imagery with a wide synoptic view of Earth has accelerated the development of Earth observation programs. Geometric modeling is an important step in maximizing the usefulness of satellite imagery. Geometric modeling of satellite imagery was started more than four decades ago. Since the launching of the SPOT satellite in 1986, many subsequent studies have attempted to implement more accurate positioning through geometric modeling. Most of the research has concentrated on satellites with pushbroom scanners such as Système Pour l'Observation de la Terre (SPOT), Indian Remote System-1C/1D (IRS-1C/1D), Modular Optoelectronic Multispectral Scanner (MOMS-02), and IKONOS [1]-[3].

Many researches point out that an obvious economic advantage of space imagery mapping over aerial imagery mapping is needed. Such an advantage should include the reduction of the density of geodetic control points. For accurate 3-D positioning using satellite images, ground control points (GCPs) play an important role. Accessibility is essential in acquiring GCP data, and this entails time and cost. Even when satellite images are available, some problems are often encountered relative to the time and cost of GCP data acquisition. For these reasons, 3-D positioning studies using ephemeris data contained in the satellite imagery can provide considerable benefit in terms of time and cost by reducing or even eliminating the need for GCPs, assuming the ephemeris information is absolutely reliable [4], [5]. However, even with these benefits, ephemeris data have a lower level of precision for accurate geometric modeling.

New and future satellite systems, like IKONOS and Quickbird, will have improved features, particularly a higher geometric resolution with a more dynamic radiometric range. In addition, the on-board Global Positioning System, inertial measurement unit, and star trackers will provide high-precision orbital positioning and attitude data. The high-precision ephemeris data permit the number of GCPs to be reduced. Furthermore, they enable georeferencing of the imagery without using GCPs. These developments present new possibilities for topographic mapping and 3-D positioning in inaccessible areas.

Korea Multi-Purpose Satellite-1 (KOMPSAT-1) was launched on 21 December 1999 by the Korea Aerospace Research Institute to address the increasing need for high-resolution satellite imagery in Korea [6]. KOMPSAT-1 electro-optical camera (EOC) produces panchromatic images with a ground sample distance of 6.6 m and a swath width of 17 km at the nadir. KOMPSAT-1 EOC uses the pushbroom mode to acquire scan line images. The launch of KOMPSAT-2 with a 1 m resolution is planned for 2004 [7], [8]. Although the KOMPSAT-1 satellite does not have the very high resolution found on such satellites as IKONOS, by utilizing ephemeris data it provides the possibility for geometric modeling without the use of GCPs.

In this study, we accomplished 3-D positioning using KOMPSAT-1 EOC imagery with ephemeris data and evaluated its accuracy. To accomplish this task, the orbital parameters for each satellite orbit, sensor attitudes, and satellite position were computed using the ephemeris data contained in the EOC imagery. Next, the actual satellite position was achieved by adjusting the offset of each satellite position. We accomplished this adjustment using only two GCPs to correct the time at the center of the image frame with respect to the ascending node. We then performed three-dimensional positioning was using stereo images with a time-adjusted satellite position. Finally, we carried out an evaluation of the accuracy of the geometric modeling using EOC images.

Table 1. Characteristics of EOC.

Characteristics	Description
Mission life time	≥3 years
Ground sample distance	6.6 m±10%
Field of view	1.42°
Swath	17 km at 685 km (nadir view)
Reliability	≥0.94
Modulation transfer function	> 10% at Nyquist frequency
Signal-to-noise ratio	≥50 over entire field of view
Focal plane array	2592 pixels
Focal length	1045 mm
Digitization	8 bits
Maximum power consumption	46 watt
Image data transmission rate	≤ 25 Mbps

II. Sensors of KOMPSAT-1

KOMPSAT-1 contains three imaging sensors: the electro optical camera, ocean scanning multispectral imager, and space physics sensor [6]. The EOC is designed for topographic mapping. With its pushbroom and body-pointing method, it provides imagery over a wide swath-width of 17 km per orbit. About 1/1024 second is required to scan one line. The ocean scanning multispectral imager is used for worldwide ocean observation, and it generates 6-band ocean color images with an 800-km swath width and a 1-km ground sample distance using whiskbroom scanning.

Table 2. Image header file data of EOC.

Parameters	Description
General parameters	Satellite name, scene ID, processing level, no. of pixels per line, no. of pixel lines per image, scene quality, etc.
General imaging data	Image orientation angle, angle of incidence, satellite altitude, etc.
Parameters for sensor modeling	Satellite position and velocity data, scene center time, sensor to body transformation data, body to flight transformation data, flight to Earth-Centered, Earth-Fixed transformation data, sensor look vectors of end detectors, detector gain, and bias data.
Orbital elements	Instantaneous field of view, field of view, viewing angle, radial speed, eccentricity, height of satellite, inclination, angular speed, argument of perigee, earth satellite distance, nominal pitch, satellite argument.

The space physics sensor, composed of a high energy particle detector and the ionosphere measurement sensor, is used for space environment monitoring. Table 1 summarizes the characteristics of the EOC used for the acquisition of the images for this study. The EOC imagery used in the study is provided in Hierarchical Data Format. The size of one scene is 2592 pixels and 2797 lines. The ephemeris data for each image are composed of general parameters, general imaging data, parameters for sensor modeling, and orbital elements, as shown in Table 2.

III. Mathematical Modeling

Some characteristics of KOMPSAT-1 compare with those of SPOT-3. KOMPSAT-1 is a rather small satellite with a mass of 500 kg operated in a sun synchronous orbit. It has a 98.46-minute orbit period, a 28-day repeating ground track, a 10:50 a.m. ascending-orbit crossing time, and a 98.13° inclination at an altitude of 685 km. On the contrary, SPOT-3 orbits at an altitude of 822 km (at the equator) with a 98.37° inclination and moves from the North Pole to the equator. KOMPSAT-1 acquires images in an ascending orbit while SPOT-3 acquires images in a descending orbit. Care needs to be taken when the image coordinate system is defined since its imaging direction is different from its counterpart.

Among the ephemeris data provided with an EOC image, some parameters used for orbit and sensor modeling include the following: latitude, longitude, and image coordinates of the center point and four corners of a scene; the image-orientation angle; angle of incidence; and sensor-look vectors of the end detectors. Ephemeris data contain information concerning the satellite position and velocity at the given ephemeris points. The position and velocity of the satellite are transmitted to the ground in an Earth-centered, Earth-fixed (ECEF) coordinate system at ¼-second intervals. Actually, position data are offered at 1-second intervals and the velocity data at ¼-second intervals. Scene center time—the scanning time for the center of an image—is presented by coordinated universal time. KOMPSAT-1 imagery has 2797 lines for one scene, so the scene center time represents the creation time of the 1398th line.

1. Orbital Parameters

Among the ephemeris information contained in a satellite image file, ephemeris data provide the satellite position, the velocity vector of the satellite at its ephemeris points, and the satellite position time at the ephemeris points from the 1950 epoch. KOMPSAT-1 gives the information for twelve ephemeris points at 1-second intervals while SPOT-3 provides them for eight points at 60-second intervals.

Using ephemeris data, orbital parameters such as the longitude of the ascending node (Ω), the argument of perigee from the ascending node (ω), orbital inclination (i), the semi-major axis of an orbit (a_s), eccentricity of an orbit (e_s), and time lapse of an orbit from ascending node to the centerline of the image frame (t_f) can be calculated, as shown in Fig. 1 [9]-[11].

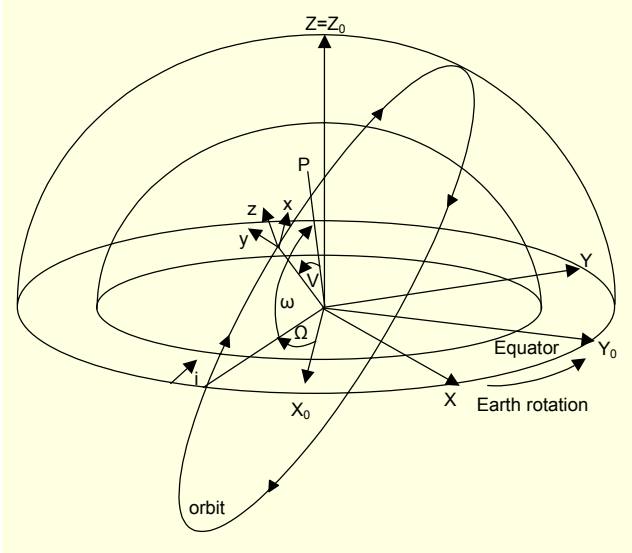

Fig. 1. Orbit of the KOMPSAT-1 satellite.

The orbital parameters were calculated using the following steps. For the ephemeris points, the measured satellite position vector $\overrightarrow{R_S}$ and velocity vector $\overrightarrow{V_S}$ are given at an instant in time referenced from a certain epoch. If we let (X_S, Y_S, Z_S) and $(\dot{X}_S, \dot{Y}_S, \dot{Z}_S)$ be the components of $\overrightarrow{R_S}$ and $\overrightarrow{V_S}$, then the magnitude of the two vectors and the magnitude of their dot product D_{RV} can be evaluated from the following equations:

$$R_s = (X_s^2 + Y_s^2 + Z_s^2)^{1/2}, \quad (1)$$

$$V_s = (\dot{X}_s^2 + \dot{Y}_s^2 + \dot{Z}_s^2)^{1/2}, \quad (2)$$

$$D_{RV} = X_s\dot{X}_s + Y_s\dot{Y}_s + Z_s\dot{Z}_s, \quad (3)$$

$$\dot{D}_{RV} = GMe(e_s \cos E)/R_s, \quad (4)$$

$$H = R_s - a_s(1-e_s^2), \quad (5)$$

$$\dot{H} = D_{RV}/R_s, \quad (6)$$

where GM_e is the Earth's gravitational constant (GM_e = 398600.5×10^9 m^3/s^2), E is the eccentric anomaly, e_s is the first eccentricity, and a_s is the semi-major axis.

The formulae for the transformation of the unit vectors $(\vec{I},\vec{J},\vec{K})$ into the converted unit vectors $(\vec{P},\vec{Q},\vec{W})$ are as follows [4]:

$$\vec{P} = C_{11}\vec{I} + C_{12}\vec{J} + C_{13}\vec{K}$$

$$\vec{Q} = C_{21}\vec{I} + C_{22}\vec{J} + C_{23}\vec{K},$$

$$\vec{W} = C_{31}\vec{I} + C_{32}\vec{J} + C_{33}\vec{K}, \tag{7}$$

$$\vec{P} = \frac{1}{GM_e e_s}(\dot{D}_{RV}\vec{R}_s - D_{RV}\vec{V}_s), \tag{8}$$

$$\vec{Q} = \frac{1}{e_s\sqrt{GM_e a_s(1-e_s^2)}}(\dot{H}\vec{R}_s - H\vec{V}_s), \tag{9}$$

$$\vec{W} = \vec{P}\times\vec{Q}. \tag{10}$$

Ω, ω, and i are calculated using (11) to (13).

$$\Omega = \tan^{-1}\left[-\frac{C_{21}}{C_{22}}\right] + \frac{\pi}{2}, \qquad 0 \le \Omega \le 2\pi, \tag{11}$$

$$i = \sin^{-1} C_{23} - \frac{\pi}{2}, \qquad 0 \le i \le \pi, \tag{12}$$

$$\omega = \tan^{-1}\left[-\frac{C_{13}}{C_{33}}\right] - \frac{\pi}{2}, \qquad 0 \le \omega \le 2\pi. \tag{13}$$

Because of the Earth's rotation, the direction of the X-axis varies for each of the ephemeris points. To use the X-axis as the reference axis through the ascending node, the correction term $\omega_e \times t$ (where ω_e is the velocity of Earth's rotation, and t is the time lapse from the ascending node to the ephemeris points) in Ω should be added in (11).

Figure 2 shows the computing procedures of the time lapse from the ascending node to the center of the image frame. The time for the center of an image and the ephemeris points can be obtained from the ephemeris data located in the satellite image file. The time length for the passage of the satellite through its perigee with respect to the 1950 epoch (t_{po}) can be written as:

$$t_{po} = t_{eo} - M_n/\omega_s, \tag{14}$$

where t_{eo} is the time lapse of the ephemeris points from the 1950 epoch, M_n is the mean anomaly, and ω_s is the satellite angular velocity, which can be calculated from the Earth's gravitational constant and the semi-major axis of the orbit. The time lapse of the ephemeris points from perigee Δt_{pe} is calculated by taking the difference between t_{po} and t_{eo}. In Fig. 2, t_{pa} represents the time of perigee from the ascending node and can be written as:

$$t_{pa} = \sqrt{\frac{a_s^{\,3}}{GM_e}} \times \left\{2\tan^{-1}\left(\frac{\sqrt{1-e_s}}{\sqrt{1+e_s}}\tan\frac{\omega}{2}\right) - \frac{\sqrt{1-e_s}\sin\omega}{1+e_s\cos\omega}\right\}. \tag{15}$$

The time of the ephemeris points from the ascending node t_{ea} is calculated by the sum of Δt_{pe} and t_{pa}. One of the orbital parameters, t_f, is calculated from the time of the center of the image and the ephemeris points obtained from the image header file relative to the 1950 epoch.

Six orbital parameters can be calculated using the ephemeris data. To calculate the ground position of any point on a satellite image, the orbital parameters for that point must be determined.

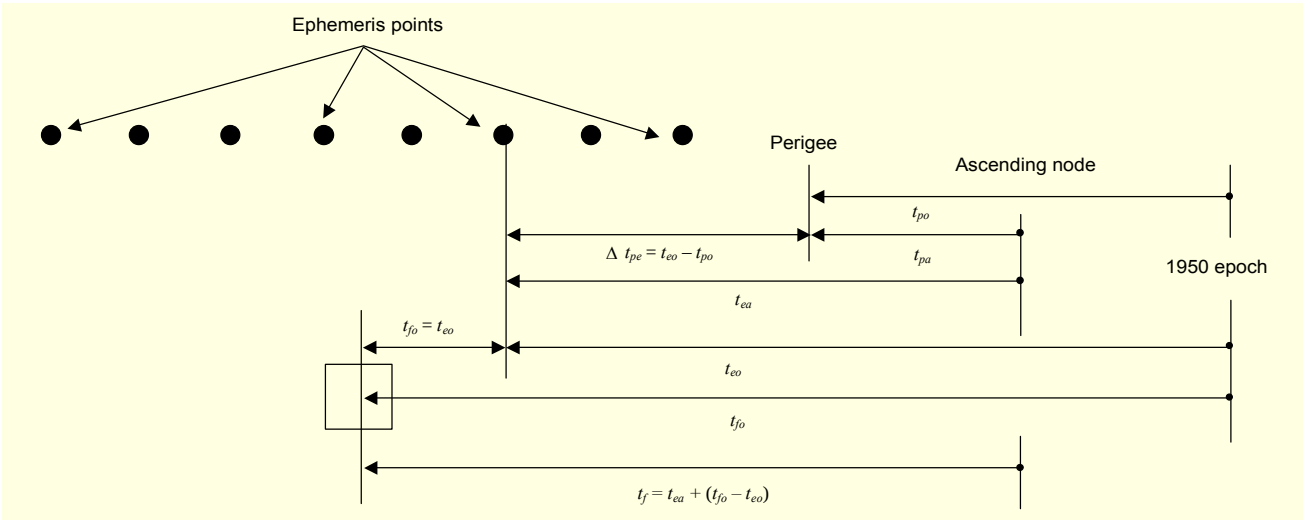

Fig. 2. Calculation of the time at the center of the image frame.

By interpolating the orbital parameters in the ephemeris points using polynomial equations represented by the time lapse of the center of the image, the orbital parameters of any point located between the ephemeris points can be formulated.

KOMPSAT-1 imagery has 2797 lines and a scanning time of 0.000976 s for one line and 2.730 s for one scene. Since the velocity of KOMPSAT-1 is 7.51 km/s, the rate of change of the orbital parameters in one scene is very small. However, for precise positioning, the orbital parameters for any point must be determined by taking these small changes into consideration.

Rotation angles for the 3-D axis of the sensor are computed using attitude data inside the ephemeris data in order to obtain the EOC attitude at the image acquisition time. The KOMPSAT-1 body has a rotating capability in the range of -45° to +45° which is used to obtain ground images. In other words, SPOT obtains its stereo images by rotating a steerable mirror in the across-orbit direction, but KOMPSAT-1 gets them by rotating the satellite body itself.

2. Geometric Modeling for 3-D Positioning

Three-dimensional positioning of KOMPSAT-1 imagery is achieved by calculating the orbital parameters of the imagery itself [4]. Errors involved in the ephemeris data are precisely modeled using GCPs, improving the accuracy of the 3-D positioning. Figure 3 gives details of the adjustment procedure.

EOC imagery is acquired using a CCD linear array in pushbroom mode, creating 2797 perspective centers in each EOC image frame. Every scan line is taken from a different position and orientation, therefore the position of any point in a scan line can be represented in a scan line coordinate system. Using this system, 2-D image coordinates (row, col) are converted into a 3-D scan line coordinate system. Consequently, a coordinate system for sensor modeling used in 3-D positioning can be obtained by converting the scan line coordinate system into a sensor coordinate system through the rotation of the tilted angle along the satellite track.

After computing the time difference between any given point and the center of an image using the image coordinates (row, col) of the given point in the sensor coordinate system, the orbital parameters and sensor attitudes for the point are computed using a polynomial equation obtained from the orbital parameter acquisition procedures.

The rotation angles were computed for each coordinate axis, allowing the Z-axis of ECEF to pass through any arbitrary point on the image by using i, ω, and Ω, among the obtained orbital parameters. The sensor rotation (roll, pitch, yaw) was added to the computed rotation angle to construct the rotation matrix R. To allow the Z-axis to pass through the perigee, true anomaly must be considered.

The actual satellite position vector $\vec{P}_{act}$ was determined by the sum of the nominal position vector $\vec{P}_{nor}$ and the satellite position offset vector Δ_s as follows:

$$\vec{P}_{act} = \vec{P}_{nor} + \Delta_s, \tag{16}$$

where the nominal position vector $\vec{P}_{nor}$ is computed using the computed rotation matrix and the radius of the satellite orbit ρ_s. The nominal position vector is influenced by irregularities in Earth's gravity, as well as by the gravitation of the moon and the sun.

The 3-D position vector of any given ground points in an ECEF coordinate system $\vec{X}$ was computed using the actual satellite position vector $\vec{P}_{act}$ the coordinate vector with the sensor coordinate system $\vec{x}$, the scale factor s, and the ground position error Δ_g, as shown in the following equation:

$$\vec{X} = \vec{P}_{act} + sR\vec{x} + \Delta_g. \tag{17}$$

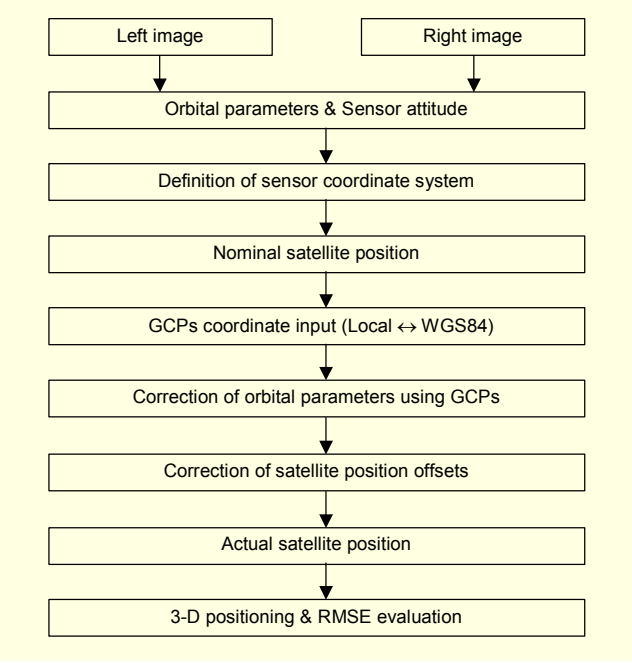

Fig. 3. Geometric modeling of KOMPSAT-1 EOC imagery.

Using GCPs located in the observed area, it was possible to correct the errors between the satellite and ground positions using a linear shift from the 3-D positioning procedures. The reference ellipsoid used for mapping purposes in Korea is Bessel (1841) while the KOMPSAT-1 system uses WGS84. When ellipsoidal heights are used as GCPs, it is sometimes necessary to transform the heights of the GCPs in the Bessel

ellipsoid to those used in the WGS84 system.

The amount of offset of the satellite position and the amount of ground position error differ from each other when stereo images are obtained from two different orbits. In this study, t_f and other orbit parameters were corrected to reduce the offset of the satellite position.

Geometric modeling is performed by correcting the orbit parameters in order to determine the actual satellite position, removing the position offset that exists between each satellite orbit track and finally obtaining the three-dimensional coordinates of the ground points, as shown in Fig. 3.

IV. Analysis and Assessment of Results

To check the accuracy of geometric modeling using KOMPSAT-1 EOC imagery, two sets of stereo images over Daejeon and the Nonsan area in Korea were used, as shown in Fig. 4. Stereo images over Daejeon were obtained from two different satellite orbit tracks with side looking angles of 4° and 26°. These two images were referred to as D04 and D26. The D04 and D26 images were set as left and right images, thus forming a stereo set. The stereo set over the Nonsan area was acquired using two images referred to as N12 and N19 with look angles of 12° and 19°. N12 and N19 formed another set of stereo images.

D04 was acquired on March 1 and D26 on March 9, 2000. N12 was obtained on April 29 and N19 on May 1, 2000. The size of each image was 2,592 × 2,796 pixels. A 1:5,000 digital map made by Korean National Geographic Information Institute (KNGII) was used to identify the GCPs and checkpoints. The accuracy of the 1:5,000 digital map is ±3.50 m in a horizontal direction and ±1.66 m in a vertical direction [12]. Figure 5 shows the selected checkpoints over the study area. Thirty five checkpoints were used for the Daejeon area while 23 checkpoints were used for the Nonsan area.

1. Analysis of Orbital Parameter Calculations

The orbital parameters for each ephemeris point were calculated using ephemeris data associated with the EOC image data. The rate of changes of the orbital parameters were very small when estimated using twelve ephemeris points. For the D04 image, t_f varied between 603.0734 and 603.0852 seconds, i fell in the range of 98.18190 to 98.18224°, Ω in the range of 136.54062 to 136.54119°, and a_s in the range of 7068.4185 to 7068.8112 km. The perigee, ω, however, showed a slightly larger rate of change (92.21437 to 93.75655°) compared with those of the other orbital parameters. Table 3 summarizes the estimated mean values of the orbital parameters for the D04, D26, N12, and N19 images.

When the orbital parameters are calculated for the twelve ephemeris points, a polynomial enables the orbital parameters

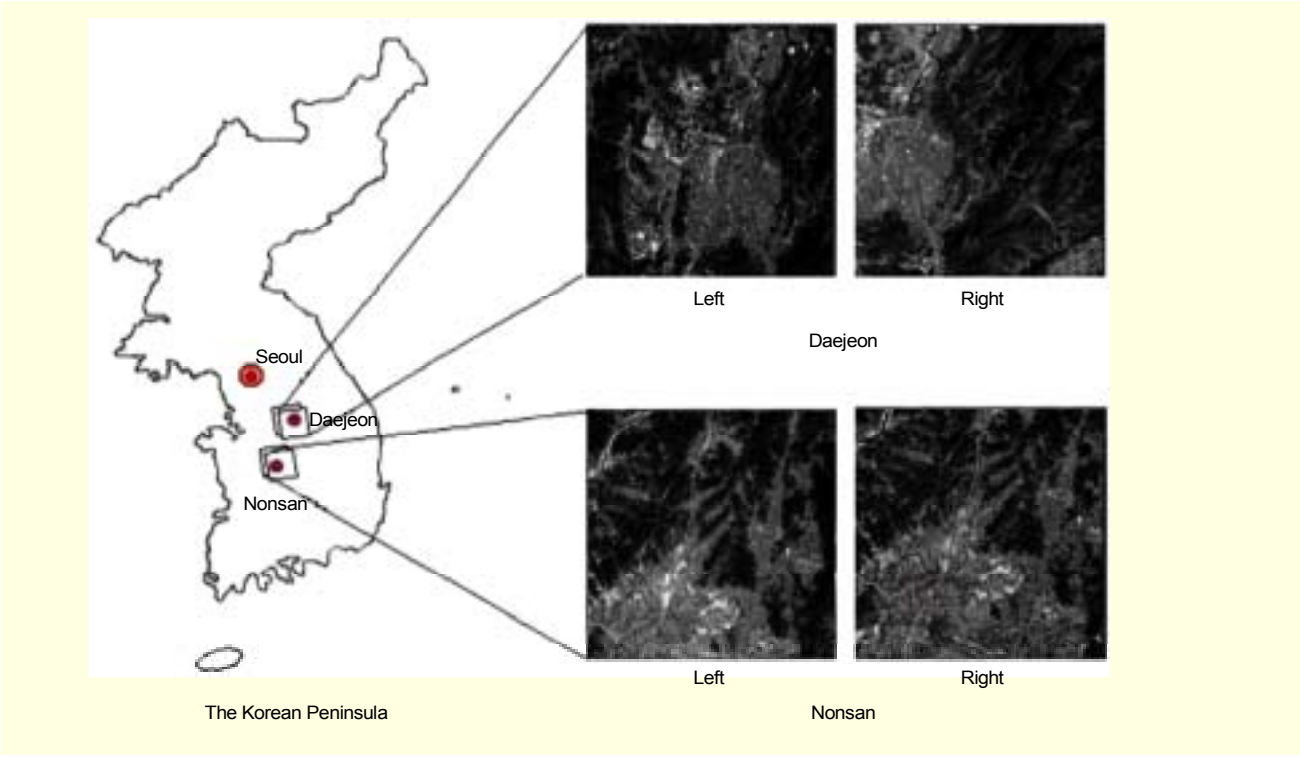

Fig. 4. KOMPSAT-1 EOC stereo images of Daejeon and Nonsan.

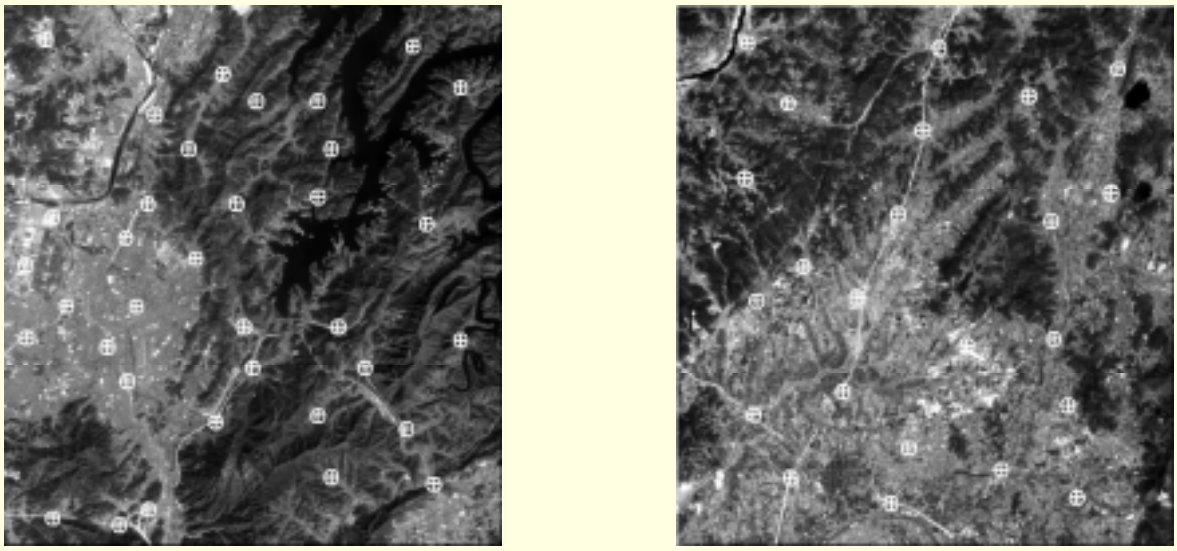

(a) Right image of Daejeon (b) Right image of Nonsan

Fig. 5. The distribution of checkpoints in the right images of Daejeon and Nonsan.

Table 3. Orbital parameters of stereo images.

		t_f (s)	i (°)	Ω (°)	ω (°)	a_S (km)	e_s
Daejeon	D04	603.0784	98.181657	136.540987	92.590228	7068.6611	0.0011905
	D26	590.5034	98.180451	132.093262	103.359450	7067.5403	0.0010194
Nonsan	N12	604.1882	98.173665	137.330939	114.911006	7065.5066	0.0014244
	N19	593.9672	98.173828	132.865088	109.514177	7066.3004	0.0013945

Table 4. Attitude of images.

		roll (°)	pitch (°)	yaw (°)
Daejeon	D04	-3.815670	-0.147880	-0.003094
	D26	25.626683	-0.187586	0.078151
Nonsan	N12	-12.164467	-0.031455	0.004412
	N19	19.242215	-0.294615	0.094367

to be computed at any given time since the rate of changes is small. Third order polynomials describe the orbital parameter in a specific time relative to the center line of the image frame. To estimate the three-dimensional rotation angles of the sensor, attitude information associated with the ephemeris data was used. For SPOT-3 imagery, ephemeris information provided the look angle. For KOMPSAT-1, however, the look angle could only be derived using attitude data. Table 4 shows the data on the calculated sensor attitude.

2. Assessment of Three-Dimensional Positioning Accuracy

Three-dimensional positions on the ground were calculated using a pair of KOMPSAT-1 stereo images obtained from two different orbits. This process was attempted using only ephemeris data, but a slight offset was found in satellite position for each orbit. We performed the geometric modeling accordingly in two steps. First, we carried out an adjustment of the offset of the satellite position for a single image in each orbit. Using the adjusted stereo pair, three-dimensional locations were subsequently calculated.

Before performing the geometric modeling of the satellite's position, special care should be taken. The ephemeris information of KOMPSAT-1 was given in the WGS84 ellipsoid model. Most of the ground control points in Korea use a height referring to the Bessel (1841) ellipsoid. It was therefore necessary to carry out a coordinate transformation from the Bessel to the WGS84 ellipsoid model. Reference [13] showed that the height difference between the two ellipsoidal

models was about 83 to 90 m in the study area.

The offsets of the satellite positions were calculated using imagery obtained over Daejeon and Nonsan, and then compared with the results using two GCPs for each set, as shown in Table 5. The absolute positional error of each offset was about 17 to 22 km when the geometric modeling was performed using only the ephemeris data of each image. The relative positional error, however, was 7 to 19 m. In this case, the relative positional errors refer to the accuracy of relative position among the checkpoints; they are not a deviation from the national datum. This confirmed that an offset in ground position exists in the geometric modeling process. When 3-D

Table 5. 3-D positioning root mean square error with ephemeris data (unit: km).

		Check points	Absolute position errors				Relative position errors (Δ P)
			Δ X	Δ Y	Δ Z	Δ P	
Daejeon	D04	35	11.2740	7.3202	17.2392	21.8604	0.0150
	D26		9.1244	5.5925	13.5831	17.2926	0.0189
Nonsan	N12	23	10.1393	4.6857	13.4505	17.4837	0.0071
	N19		11.7124	5.9553	16.1370	20.8099	0.0191

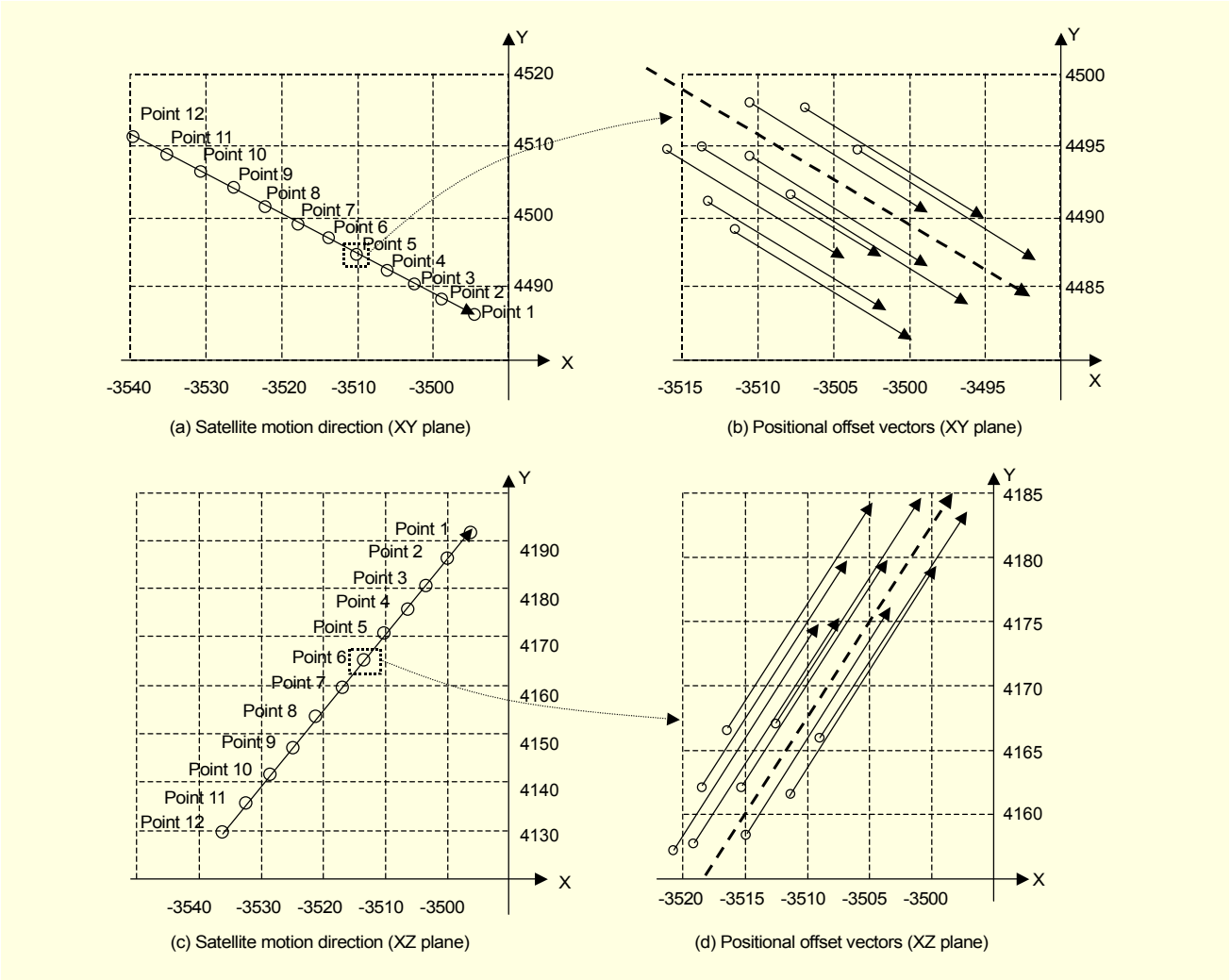

Fig. 6. Satellite motion direction and positional offset vectors.

positioning was checked using D04 (left image of Daejeon), a constant offset of the satellite's position was found along the satellite's orbital track, as shown in Fig. 6.

Figures 6(a) and 6(c) show the array for 12 ephemeris points. The solid lines in Fig. 6(b) and 6(d) represent the magnitude and direction of the positional errors of the checkpoints, while dotted lines indicate the direction of the satellite track. Similar trends were found for each of the other three images. The offset can be considered a significant positional error in terms of absolute positioning. The error of relative positioning, on the other hand, was small. We assume that the constant shifts were caused by inconsistencies between the time of the center of the image frame and the ephemeris points provided by the ephemeris data. We performed the procedure for adjusting the orbital elements in two steps. First, we calculated the 3-D coordinates of the checkpoints using the ephemeris data only. Second, we performed iteration until the offsets from the actual coordinates in X, Y, and Z directions were minimized by adjusting the orbital elements.

Using the ground control points, we adjusted the time difference between the center of the image frame and the ephemeris points, and updated the other orbit parameters accordingly. Out of the many checkpoints distributed over the images, only one or two were selected for use as GCPs in adjusting the satellite's positional offset. Figure 7 shows the patterns of GCP distribution used in the adjustment.

Table 6 shows the magnitude of correction for t_f. The deviation in the correction was very small regardless of the number and distribution of the GCPs shown in Fig. 7. Thus, it would appear that one ground control point was sufficient to adjust t_f. However, two control points, such as in case 6 in Fig. 7, were used to reduce the positioning error propagated in the across direction of the track by side looking to acquire the stereo images. In general, using case 6 presents more accurate results than using the other cases in three dimensional positioning.

Table 7 shows the magnitude of the corrections for the orbital parameters when two ground control points were used. Different amounts of correction were evident from scene to scene, since each image was obtained in a different orbit.

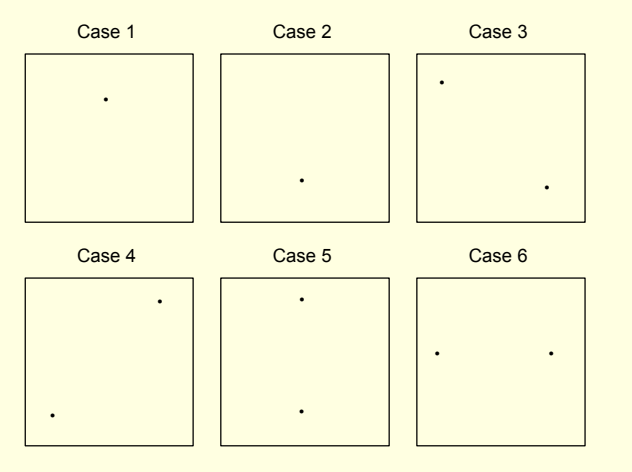

Fig. 7. Patterns of GCPs used for adjusting the satellite's positional offset.

Table 6. The correction amount for the time of the image center.

Case	t_f corrections	Correction deviation
1	3.1833 s	0.0041 s
2	3.1838 s	
3	3.1861 s	
4	3.1872 s	
5	3.1870 s	
6	3.1853 s	

By determining the actual satellite position using the adjusted value of t_f, it was possible to remove the offset of the ground position along the satellite track. Successful 3-D positioning was performed from a set of stereo images since the offsets of the satellite position present in each scene were removed. However, even though the offsets were removed, ground

Table 7. Values of the orbital parameter correction using GCPs.

		Δt_f (s)	i (°)	Ω (°)	ω (°)	a_s (km)	e_s
Daejeon	D04	3.185300	-0.000057	-0.000001	0.603496	-0.158500	-0.000013
	D26	2.529100	-0.000115	-0.000459	0.505350	-0.116600	-0.000016
Nonsan	N12	2.547200	-0.000057	-0.000115	0.249925	-0.033000	0.000002
	N19	3.038300	-0.000065	-0.000058	-0.175608	0.035200	-0.000002

Table 8. 3-D positioning error of EOC stereo images.

CASE	Area	Check points	Positional errors (RMSE) (unit: km)			
			ΔX	ΔY	ΔZ	ΔP
1	Daejeon	35	0.0165	0.0103	0.0125	0.0231
	Nonsan	23	0.0153	0.0097	0.0131	0.0229
2	Daejeon	35	0.0146	0.0116	0.0095	0.0209
	Nonsan	23	0.0157	0.0103	0.0184	0.0263
3	Daejeon	35	0.0129	0.0101	0.0103	0.0194
	Nonsan	23	0.0129	0.0027	0.0109	0.0171
4	Daejeon	35	0.0141	0.0141	0.0083	0.0216
	Nonsan	23	0.0080	0.0025	0.0086	0.0120
5	Daejeon	35	0.0177	0.0116	0.0111	0.0239
	Nonsan	23	0.0154	0.0093	0.0098	0.0205
6	Daejeon	35	0.0095	0.0105	0.0094	0.0170
	Nonsan	23	0.0083	0.0027	0.0083	0.0120

positional errors remained. These errors were larger across the track than along the track. Table 8 shows the errors in ground position depending on the number of GCPs used and their distribution. The overall accuracy improved when two ground control points were used rather than one. Case 6 obtained the best results, which had a 12–17 m root mean square error (RMSE), as shown in Table 8. The effect of the side-looking geometry was minimized using this GCP distribution.

V. Conclusion

Three-dimensional positioning using a traditional photogrammetric approach with ground control points can be both time consuming and costly, particularly with regard to collecting GCPs. Furthermore, problems arise when 3-D positioning or topographic mapping is needed for an inaccessible area. Geometric modeling using only ephemeris data or a minimum number of GCPs can be beneficial in terms of time and cost. This study confirmed the possibility of geometric modeling using only ephemeris data obtained from KOMPSAT-1 EOC imagery. KOMPSAT-1 was the first Korean satellite to be used for topographic mapping.

Orbital parameters, sensor attitudes, and the satellite position for each satellite orbit were computed using ephemeris data. After estimating the orbital parameters for twelve ephemeris points, we found the rates of change for the orbital parameters to be very small. The argument of perigee, however, showed a slightly larger rate of change compared with those of the other orbital parameters.

We made an attempt to determine the satellite position using only ephemeris data. However, an offset of the satellite position was found to exist for each orbit. Geometric modeling was accordingly carried out relative to the adjustment of the offset of the satellite position. The actual satellite position was achieved by adjusting the offset of the satellite position for each orbit and correcting the orbital parameters using only two GCPs.

Finally, we successfully obtained 3-D positioning from the set of stereo images since the satellite positional offsets were removed. The error in the positioning of the ground points was greater across the track than along it. By adjusting the ground positional error, we acquired 3-D positioning with an accuracy of 12–17 m RMSE, using only two GCPs in the across track direction. In the future, accurate 3-D positioning using only ephemeris data may be possible if high-precision ephemeris data can be provided by high-resolution satellites.

References

[1] D.J. Gugan and I.J. Dowman, "Topographic Mapping from SPOT Imagery," *Photogrammetric Engineering and Remote Sensing*, vol. 54, no. 10, 1998, pp. 1409-1414.

[2] A.B. Orun and K. Natarajan, "A Modified Bundle Adjustment Software for SPOT Imagery and Photography: Tradeoff," *Photogrammetric Engineering and Remote Sensing*, vol.60, no.12, 1994, pp. 1431-1437.

[3] C. Lee, H.J. Theiss, J.S. Bethel, and E.M. Mikhail, "Rigorous Mathematical Modeling of Airborne Pushbroom Imaging Systems," *Photogrammetric Engineering and Remote Sensing*,

vol. 66, no.4, 2000, pp. 385-392.
[4] S.A. Makki, *Photogrammetric Reduction and Analysis of Real and Simulated SPOT Imageries*, Ph.D. Thesis, Purdue University, West Lafayette, Indiana, 1991.
[5] D. Fritsch and D. Stallmann, "Rigorous Photogrammetric Processing of High Resolution Satellite Imagery," *Int'l Archives of Photogrammetry and Remote Sensing*, vol. B1, 2000, pp. 313-321.
[6] KARI, About KOMPSAT-1, URL: http://kompsat.kari.re.kr/english/index.asp/, 2000.
[7] Byoung-Sun Lee, Jeong-Sook Lee, Jae-Hoon Kim, Seong-Pal Lee, Hae-Dong Kim, Eun-Kyou Kim, and Hae-Jin Choi, "Operational Report of the Mission Analysis and Planning System for the KOMPSAT-1," *ETRI J.*, vol. 25, no. 5, 2003, pp. 387-400.
[8] Hee-Sook Mo, Ho-Jin Lee, and Seong-Pal Lee, "Development and Testing of Satellite Operation System for Korea Multipurpose Satellite-I," *ETRI J.*, vol. 22, no. 1, 2000, pp. 1-11.
[9] V.A. Chobotov, *Orbital Mechanics*, 2nd ed., American Institute of Aeronautics and Astronautics, Inc., 1996.
[10] P.R. Escobal, *Methods of Orbit Determination*, Krieger Publishing Company, 1975.
[11] C.C. Slama, *Manual of Photogrammetry*, 4th ed., American Society of Photogrammetry, 1980.
[12] NGII, http://www.ngi.go.kr/index_home.jsp.
[13] S.B. Lee, "Development of the Geoid Model in Korean Peninsula Referred to Bessel Ellipsoid," *J. of the Korean Society of Geodesy, Photogrammetry, and Cartography*, vol. 16, no.2, 1998, pp. 213-223.

Hong-Gyoo Sohn received the BS and MS degrees in civil and environmental engineering from Yonsei University, Seoul, Korea in 1985 and 1987. He received the PhD degree in geodetic science from Ohio State University in 1996. From 1996 to 2000, he worked as a Research Scientist at the Byrd Polar Research Center of Ohio State University. During that time he was involved in several NASA sponsored projects including the creation of a mosaic of Greenland using an old spy satellite of the 1960s and a surface change detection program using spaceborne satellite imagery. He also served as a Team Leader for the Radarsat Antarctic Mapping Project, for which he received the Group Achievement Award from NASA. He joined the School of Civil and Environmental Engineering at Yonsei University in 2000 and has been teaching GPS, GIS, and remote sensing. His research interests include surface reconstruction using airborne and spaceborne imagery, dynamic modeling of structures using GPS, and devising a disaster monitoring system in a real-time basis using SAR imagery. He is a Member of the American Society of Photogrammetry and Remote Sensing.

Hwan-Hee Yoo is a Professor and Head of the Department of Urban Engineering at Gyeongsang National University (ERDI), Jinju, Korea. He received the BS degree from Kangwon National University in 1981, and the MS and PhD degrees in civil engineering from Yonsei University, Korea in 1983 and 1988. His current research interests include modeling and the integration of satellite multisensor data as well as mapping using a videographic system.

Seong-Sam Kim received the BS and MS degrees in urban engineering from Gyeongsang National University, Jinju, Korea, in 2000 and 2002. He is currently a PhD student of the same university. His current research interests include satellite sensor modeling and multi-resolution data registration.